





Article

# The Response of Soil CO<sub>2</sub> Efflux to Water Limitation Is Not Merely a Climatic Issue: The Role of Substrate Availability

Giovanbattista de Dato <sup>1,\*</sup> , Alessandra Lagomarsino <sup>2</sup>, Eszter Lellei-Kovacs <sup>3</sup>,  
Dario Liberati <sup>4</sup> , Renée Abou Jaoudé <sup>4</sup>, Rosita Marabottini <sup>4</sup>, Silvia Rita Stazi <sup>4</sup> ,  
Gabriele Guidolotti <sup>5</sup>, Edit Kovacs-Lang <sup>3</sup>, György Kroel-Dulay <sup>3</sup> and Paolo De Angelis <sup>4</sup> 

<sup>1</sup> Council for Agriculture Research and Economics, Centre for Forestry and Wood (CREA-FL),  
Viale Santa Margherita 80, 52100 Arezzo, Italy

<sup>2</sup> Council for Agriculture Research and Economics, Research Centre for Agriculture and  
Environment (CREA-AA), Via di Lanciola 12, 50125 Firenze, Italy; alessandra.lagomarsino@crea.gov.it

<sup>3</sup> Hungarian Academy of Sciences, Centre for Ecological Research Institute of Ecology and Botany,  
H-2163 Vácraót, Hungary; lellei-kovacs.eszter@okologia.mta.hu (E.L.-K.);  
lang.edit@okologia.mta.hu (E.K.-L.); kroel-dulay.gyorgy@okologia.mta.hu (G.K.-D.)

<sup>4</sup> University of Tuscia, Department for Innovation in Biological, Agro-food and Forest systems (DIBAF),  
Via S. Camillo de Lellis snc, 01100 Viterbo, Italy; darioliberati@unitus.it (D.L.);  
renee.aboujaoude@gmail.com (R.A.J.); marabottini@unitus.it (R.M.); srstazi@unitus.it (S.R.S.);  
pda@unitus.it (P.D.A.)

<sup>5</sup> National Research Council of Italy (CNR) Institute for Agro-Environment and Forest Biology (IBAF),  
Via Salaria km 29,300, 00015 Monterotondo Scalo, Italy; gabriele.guidolotti@ibaf.cnr.it

\* Correspondence: giovanbattista.dedato@crea.gov.it; Tel.: +39-0575-353021

Academic Editor: Timothy A. Martin

Received: 22 April 2017; Accepted: 4 July 2017; Published: 7 July 2017

**Abstract:** Water availability, together with temperature, represents the most limiting abiotic factor regulating soil CO<sub>2</sub> efflux (SR). Besides the direct effect of water limitation, drought also influences plant activity, determining changes in the quality and quantity of root exudates, thus indirectly affecting soil microbial activity. To determine how the seasonal changes of plant activity and soil microbial metabolism and structure affect SR response to drought, we investigated the correlation between leaf gas exchange, soil carbon pools and soil respiration sources and the role of soil carbon pools on microbial populations and soil respiration, in a summer deciduous Mediterranean (SDS) and a winter deciduous temperate (WDS) shrublands, experiencing a dry summer period. In both sites, drought reduced photosynthesis, but affected SR differently: in SDS, SR decreased, although microbial heterotrophic respiration (SR<sub>h</sub>) remained unchanged; in WDS, SR did not vary but SR<sub>h</sub> was reduced. While in SDS the microbial community was able to respire more complex substrates, in WDS it was strongly dependent on easily decomposable molecules, thus on plant activity. Therefore, the response of soil CO<sub>2</sub> efflux to water limitation is not exclusively influenced by climate as it is modulated by the degree of adaptation of the microbial community to drought.

**Keywords:** soil CO<sub>2</sub> efflux; drought; microbial community; substrate availability; photosynthesis; heterotrophic respiration

## 1. Introduction

Water availability is a key driver of biogeochemical processes in all terrestrial ecosystems, especially in arid and semi-arid ones, which are very sensitive to climatic variation [1]. In these ecosystems, both carbon assimilation (photosynthesis) and soil CO<sub>2</sub> efflux (i.e., soil respiration, SR)

are driven by the seasonal changes in the precipitation regime [2–5]. It is supposed that the impact of water limitation can be longer lasting on assimilation than on soil CO<sub>2</sub> efflux [6], due to the likely different capacity of leaves (and consequently canopy) to reverse to pre-drought conditions compared to microorganisms' ability [7–9]. However, as soil respiration represents one of the largest fluxes of CO<sub>2</sub> [10], it is essential to determine how water availability directly and indirectly affects carbon release from the perspective of climate change.

Soil CO<sub>2</sub> efflux (SR) results from the respiratory activity of the autotrophic and heterotrophic components of the pedosphere, deriving from both plant (root respiration) and microorganisms (microbial respiration; [11]). The contribution of microbial respiration in different ecosystems can account for 10–90% [12,13] of the total CO<sub>2</sub> efflux, depending on biotic (plant community, phenological stage, relative contribution of coarse and fine roots, microbial biomass and community; [14–16]) and abiotic factors (climatic drivers, soil conditions, such as pH and soil structure, topography, sampling period, management type; [17–19]).

Several studies show that the microbial community structure and activity can vary according to plant activity [20], as long as there are labile soil carbon inputs and available substrates [21,22]. In fact, plants sustain soil CO<sub>2</sub> efflux by “pumping” fresh carbon assimilated via photosynthesis to roots, therefore feeding roots and the microorganisms inhabiting the narrow region of soil that is directly influenced by root secretions (plant assimilates and rhizodepositions), the so-called rhizosphere [23–25]. Thus, the contribution of this root-derived CO<sub>2</sub> is strongly dependent on plant activity, decreasing during plant dormant periods or under stress conditions and increasing during the non-moisture limited growing period.

Microbial activity is strongly controlled by temperature but other constraints can modify the temperature response, by altering the microbial structure and function [26].

Especially when water availability is the most limiting environmental factor, due to a combination of high temperatures and low rainfall, the physiological performance of soil fauna can be directly and indirectly reduced, subjecting the microbial community to strong adaptive adjustments [27].

Microbial communities and functionality show elevated plasticity in terms of composition, diversity and physiological modifications. According to Allison and Martiny [28], microbial communities can be resistant to environmental changes, remaining unaltered, but they can also exhibit resilience and quickly return to their original state after a disturbance; further, there are cases showing redundancy, consisting in microbial composition changes but unaffected functionality.

These observations become particularly evident under drought conditions, when bacterial community assortments show higher diversity compared to wet conditions, highlighting the role of rainfall regime in determining soil microbial properties [29,30]. According to frequency and intensity of drought events, microbial structure may be selected towards groups that are more tolerant to desiccation. Moreover, different drought patterns may result in different community assemblages of functional groups, able to differently respond to moisture stress [31], and to regulate heterotrophic respiration [32–35]. This microbial behaviour appears particularly striking in a Mediterranean climate, where the intense seasonality of soil water availability and temperature, in the long run, may have selected microbial communities able to tolerate this strong seasonal shift [36].

In order to determine how the response of SR to drought can be modulated by plant activity and soil microbial characteristics, we analysed the seasonal change of: (1) plant performances (assimilation, stomatal conductance) and water status (pre-dawn water potential); (2) soil CO<sub>2</sub> efflux and its components; and (3) substrate availability (soil carbon pools, water-extractable organic carbon); (4) microbial activity (by induced respiration) and composition (by ester-linked fatty acid methyl ester-EL-FAME), analysing relationship between leaf gas exchange, soil carbon pools and soil respiration sources and the role of soil carbon pools on microbial populations and soil respiration. We monitored two different sites: a summer deciduous Mediterranean and a winter deciduous temperate shrubland experiencing a dry summer period.

## 2. Materials and Methods

### 2.1. Study Site

The Italian site (Table 1; Figures A1 and A2) is located in the Regional Park Porto Conte-Capo Caccia in northwest Sardinia, Italy. The climate of the area is Dry Thermo-Mediterranean [37] with the dry period extending from May to September. The soil is rocky and shallow; the texture is sandy loam, with an ABC profile. Vegetation cover is a typical Mediterranean shrubland made up of plants with 1 m maximum height, constituted of *Cistus monspeliensis* L., *Helichrysum italicum* G. Don. and *Dorycnium pentaphyllum* L. As with many summer semi-deciduous plants, *Cistus* is characterised by a drought-avoiding phenology, with summer leaf shedding. Hereafter, this site will be referred to as summer deciduous shrubland (SDS).

**Table 1.** Main characteristics of the study areas. The two values of air temperature and precipitation refer to the 30-year average measured in a proximal meteorological station and to the 2010 values measured at the study site.

	Hungary (WDS)	Italy (SDS)
Location	46°53' N, 19°23' E	40°36' N, 8°9' E
Altitude (m)	108	35
Air temperature (°C)	<u>30-year/2010</u>	<u>30-year/2010</u>
Annual	10.6/10.3	16.8/16.3
July	21.1/22.2	29.9/24.5
January	−1.9/−2.2	6.7/10.0
Precipitation (mm year <sup>−1</sup> )	<u>30-year/2010</u>	<u>30-year/2010</u>
	505/1026	643/824
Main growing season(s) > 5° more than 5 days	April–September	March–June October–December
PET potential evapotranspiration (mm)	914	1026
AET actual evapotranspiration (mm)	203	246
GDD (°C) (5 < T < 25) growing degree days	2386	3180
<b>Soil Characteristics</b>		
Soil type (FAO standard)	Calcaric Arenosols	Luvi and Leptosols
Top soil		
Depth (cm)	0–10	0–20
pH	7.9	7.7
C/N	14.3	34
SOM (%)	0.74	3.8
Bulk density (g cm <sup>−3</sup> )	1.4	1.1
Deeper soil		
Depth (cm)	10–20	20–40
pH	8.1	7.8
C/N	6.7	52
SOM (%)	0.32	4.7
Bulk density (g cm <sup>−3</sup> )	1.45	1.1
Plants		
Dominant Plant species	<i>Populus alba</i> <i>Festuca vaginata</i> <i>Cynodon dactylon</i> <i>Stipa borysthena</i>	<i>Cistus monspeliensis</i> <i>Helichrysum italicum</i> <i>Dorycnium pentaphyllum</i>
Plant cover (%)	35	82
Main rooting depth	0–20	0–10

The Hungarian site (Table 1; Figures A1 and A2) is located in the Kiskunság National Park. The climate is Pannonian—a temperate climate with continental and sub-Mediterranean influence [38], with cold winters and warm, dry summers. Peak precipitation usually occurs in June, often followed by a midsummer drought. Soil of the Kiskunság region is Pleistocene sand from the River Danube. The coarse sandy soil, very poor in organic matter (<1%), is mainly in the upper 0–10 cm horizon and has an extreme heat and water regime. The vegetation is characterized by the presence of a forest–steppe transitional biome. The dominant species are the winter deciduous clonal *Populus alba* L. and the perennial C<sub>3</sub> bunchgrass *Festuca vaginata* W. et K. In the warm and dry summers the activity of C<sub>3</sub> grasses decreases, while the activity of poplar clones is continuous during the vegetation period. Hereafter, this site will be referred to as winter deciduous shrubland (WDS).

We sampled at three occasions during 2010, under different conditions of water availability, soil temperature and plant phenological status: in Italy, the three campaigns were in March, August and October; in the Hungarian site the campaigns were in May, July and November. The different timings will be named Spring, Summer and Autumn in the following text. These campaigns were chosen in order to find comparable climatic conditions but different phenological stages (Table 2).

**Table 2.** General characteristics of climatic conditions (soil water content (SWC) and temperature), phenological status (vegetative period) and related source of C for soil CO<sub>2</sub> efflux (PI = CO<sub>2</sub> from plant activity, i.e., sustained by plant photosynthesis; SOM = CO<sub>2</sub> from soil organic matter).

	Spring		Summer		Autumn	
	WDS	SDS	WDS	SDS	WDS	SDS
SWC	not limiting	not limiting	limiting	limiting	not limiting	not limiting
Temperature	not limiting	not limiting	not limiting	not limiting	limiting	not limiting
Vegetative period	active	active	active	not active	not active <sup>1</sup>	active
Source of C	PI + SOM	PI + SOM	PI + SOM	SOM	PI + SOM	PI + SOM

<sup>1</sup> Autumn is not an active period in Hungary (WDS) for poplars and C<sub>4</sub> plants in dormant status, while the C<sub>3</sub> plants (*Festuca vaginata*) are inactive only in frosty or snow-covered winter periods.

All the measurements described below were taken, during the different campaigns, on the same ten dominant individuals of *C. monspeliensis* in SDS and *P. alba* in WDS and on the soil around the canopy of these plants.

## 2.2. Leaf Gas Exchange and Pre-Dawn Water Potential

Plant activity and water status were determined by measuring photosynthesis ( $A_{net}$ ), stomatal conductance ( $g_s$ ) and pre-dawn leaf water potential (PWP).

Due to differences in leaf shape of the two analysed species,  $A_{net}$  was measured by Li-6400 (Licor Biosciences, Inc., Lincoln, NE, USA), equipped with 6400-02B LED light source during the Hungarian campaigns, and with the 6400-22L Package (which combines the 6400-22 Opaque Conifer Chamber and the 6400-18 RGB Light Source) during the Italian ones. Photosynthesis was measured on attached leaves of 10 dominant plants at midday. The cuvette was conditioned according to the season by setting the internal values of the photon flux density (PAR), the relative humidity and the air temperature equal to the external values (Table A1), while [CO<sub>2</sub>] was always set to 400 ppm. Leaf area clipped during the Hungarian campaigns was equal to the chamber area (6 cm<sup>2</sup>), being the cuvette totally filled in with the poplar leaves; in the Italian site, *Cistus* shoots were cut after each measurement and leaves were scanned.

At each sampling date, pre-dawn leaf water potential was measured by the pressure bomb SKPM 1400 (Skye Instruments Ltd, Llandrindod Wells, UK) on *C. monspeliensis* shoots in SDS, because of the lack of an evident petioles, while in WDS it was measured on poplar leaves. The measurements were done on one sample per plant. The shoots were cut and put in plastic bags in an insulated box and measured within some minutes.

### 2.3. Soil CO<sub>2</sub> Efflux

Soil CO<sub>2</sub> efflux (SR) was measured on fixed PVC collars (one collar next to each of the 10 dominant individuals, inserted into the soil for 5 cm at a distance from the plant base of 30–50 cm under the projection of the plant canopy) by Licor 8100 (Licor Biosciences, Inc., Lincoln, NE, USA) equipped with the 8100–102 (10 cm) chamber. The collars were installed a couple of days prior the start of each measurement campaign and kept free of vegetation.

The Soil Temperature Probe Type E (Licor Biosciences, Inc., Lincoln, NE, USA) was used to measure soil temperature (Ts) at each sampling point. Soil water content at the time of measurements was determined on a soil sub-sample deriving from the soil cores collected inside each collar and used for the determination of the heterotrophic component of SR (SR<sub>h</sub>, see below) in the laboratory. These sub-samples were dried in an oven at 110 °C until they reached constant weight.

### 2.4. Soil Heterotrophic Respiration, Heterotrophic Basal Respiration and Temperature Sensitivity

After SR measurements, one soil core (mineral layer 0–5 cm) inside each collar was collected. The cores were sampled by an undisturbed soil corer (07.53.SC, Eijkelkamp Soil & Water, Giesbeek, The Netherlands), having an area of 19.63 cm<sup>2</sup> (ø 5 cm) and height of 5 cm. After sampling, cores were stored at 5 °C for 2–3 days until performing the incubation in the laboratory, in order to exclude from the measurement the contribution of the autotrophic component of CO<sub>2</sub> efflux and to minimize the decomposition of dead roots [39].

The incubation was performed by a water bath (Haake, type Q with F3 digital controller) equipped with a tank. Soil cylinders were inserted into plastic glasses (ø 6 cm), which were attached to the bottom part of the tank lid and dipped into the water flowing in the tank. Attached on the top of the lid, concentric to the holes for soil cylinders, plastic rings (ø 10 cm) were placed, in order to fit the Licor 8100–102 chamber connected to a Licor 8100 (Licor Biosciences, Inc., Lincoln, NE, USA), used for CO<sub>2</sub> efflux measurements. Soil temperature was monitored by thermocouples (Tecno.el, s.r.l., Formello, Roma, Italy) connected to a datalogger (CR10X, Campbell Scientific, Inc., Logan, UT, USA). After the soil had reached the desired temperature (Ts of 5–10–15–18–20–25–30 °C, and midday field soil temperature, therefore varying with the seasons and defined as actual soil temperature), we started CO<sub>2</sub> efflux measurements in 20–30 min. CO<sub>2</sub> efflux measurement at field temperature was used to determine the heterotrophic respiration (SR<sub>h</sub>). Heterotrophic respirations at the different temperature steps were fitted by the exponential equation  $SR_h = a \cdot \exp(k \cdot Ts)$  (Equation (1)), where SR<sub>h</sub> is the heterotrophic soil CO<sub>2</sub> efflux, a and k are estimated parameters, and Ts is the soil temperature. From these curve, we derived the heterotrophic basal respiration SR<sub>b</sub> = a for Ts = 0 °C, and the temperature coefficient of the heterotrophic respiration  $Q_{10} = \exp(10 \cdot k)$ .

### 2.5. Soil C Pools

Total soil Organic (TOC) and total N (TN) were determined at the beginning of the campaigns (in spring) in the bulk (non-fractionated) soil and in particle and aggregate-size fractions. Between 20 and 40 mg oven-dried material of each unit was weighed into AGram–foil capsules. The method was based on dry combustion using an elemental analyser (FlashEA 1112, Thermo Fisher Scientific Inc., Waltham, MA, USA).

Water-extractable organic carbon (WEOC) was determined after extraction of 15 g of soil in 30 mL of deionised cold water. Total C in the aqueous extracts was measured by dry combustion on a C and N soil analyser Flash 2000 Series (Thermo Fisher Scientific Inc.).

### 2.6. Community Level Physiological Profiles (CLPP) Based on Substrate-Induced Respiration (SIR)

Microbial activity was determined by analysis of CLPP using the MicroResp soil respiration system (MicroResp™ Macaulay Scientific Consulting Ltd., Aberdeen, UK), as described in Campbell et al. [40] and Lagomarsino et al. [39]. Mineralization of 15 carbon substrates was tested for CLPP (Table A2):

five carbohydrates (glucose, galactose, fructose, arabinose, trehalose); five amino acids (lysine, alanine,  $\gamma$ -aminobutyric acid, arginine); four carboxylic acids (citric acid, oxalic acid, ascorbic acid, malic acid); and one amide (N-acetyl-glucosamine). Carbon substrates were selected depending on their ecological relevance to soil and their similarity to substrates used for enzyme activities. In particular, rhizospheric sources (carboxylic acids and carbohydrates) were chosen considering the importance of root inputs for microbial metabolism.

The sources were dissolved in deionised water and added before the soil to ensure that the soil contacted the source at the same time for all wells. For each soil a water control was present in the plate. To obtain the substrate induced respiration (SIR), the soil respiration values for the various carbon sources were adjusted by subtracting the average value of the water control. Three laboratory replicates were used for each field replicate. To estimate the evolved CO<sub>2</sub>, a colorimetric method relying on the change in the pH of a gel-based solution of bicarbonate was used. The absorbance at 590 nm was read with a Biolog MicroStation (Microlog™ Release 4.20.04, Biolog, Inc., Hayward, CA, USA) immediately before and after 6 h of incubation at 28 °C. The absorbance after 6 h was normalized for any differences recorded at time zero and then converted to % CO<sub>2</sub> by using the following calibration curve:  $y = A + B/(1 + D \times A_i)$ , where  $A = -0.3409$ ,  $B = -1.4604$ ,  $D = -7.882$  and  $A_i$  is the absorbance at 590 nm. The % CO<sub>2</sub> was then converted to  $\mu\text{g CO}_2 \text{ g}^{-1} \text{ h}^{-1}$  production rate using gas constant,  $T$  (°C), soil d.w. (g) and the incubation time (hour) (Table A1).

### 2.7. Microbial Community Composition by EL-FAME Characterization

Microbial community structure was characterized by ester-linked fatty acid methyl ester (EL-FAME) analysis, which employed a mild alkaline methanolysis method to extract ester-linked (EL) fatty acids but not free fatty acids [41]. In brief, 16.6 mL of 0.2 M potassium hydroxide (KOH) in methanol and 5  $\mu\text{L}$  of internal standard solution (0.023 mg mL<sup>-1</sup> methylnonadecanoate 19:0) were added to a 50-mL centrifuge tube containing 5 g of freeze-dried soil. The tubes were incubated at 37 °C for 1 h in an orbital shaker. Then 6.6 mL of 1.0 M acetic acid were added to neutralize the pH of the tube contents. Extracted FAMES were partitioned into an organic phase by adding 10 mL of hexane followed by centrifugation at 4500 rpm for 15 min. The hexane layer was transferred into a clean glass tube, dehydrated with Na<sub>2</sub>SO<sub>4</sub>, filtered and evaporated under a steam of N<sub>2</sub>. Finally, FAMES were dissolved in 200  $\mu\text{L}$  of dichloromethane and transferred to an amber vial for GCMS analysis for quantification. Mass spectra were recorded by the use of a QP-5050 (Shimadzu, Kyoto, Japan) spectrometer equipped with an AT 20 capillary column (0.25 mm i.d., 25 m) (Alltech, Nicholasville, KY, USA) at 80–280 °C with a splitless injection and an isothermal program at 89 °C for 2 min, then 6 °C min<sup>-1</sup> up to 280 °C and finally isothermal at 280 °C for 5 min. Methylated fatty acids were identified according to their mass spectra and using BAME 24 (47080 U) and 37 FAME Mix (47885-U, Sigma-Aldrich) as chemical standards.

Standard nomenclature is used to describe FAs (Table A3), which are designated by the total number of carbon atoms/number of double bonds, followed by the position of the double bond from the methyl (aliphatic) end ( $\omega$ ) of the molecule. The prefixes “a” and “i” refer to anteiso- and iso-branched FAs. The prefix “10Me” indicates a methyl group on the tenth carbon atom from the carboxyl end of the molecule and “cy” indicates cyclopropane FAs. Biomarkers of specific functional groups were assigned according to Table A2 reporting the classification used. Total bacteria were calculated as the sum of Gram+ (G+), Gram– (GRAM–), General and Actinomycetes.

### 2.8. Statistical Analysis and Functional Diversity Calculation

Temporal variation of CO<sub>2</sub> assimilation, pre-dawn water potential, soil CO<sub>2</sub> efflux, water soluble carbohydrates, EL-FAMES and induced respiration was detected by analysis of variance (ANOVA) separately for the two sites with season as the independent variable.

Correlations among the fluxes with biotic and abiotic variables were performed.

The responses of microbial population to substrates (CLPPs data) and population structures (EL-FAME data) to sampling time and abiotic factors were analysed by Principal Component Analysis (PCA). Dependent data are expressed as relative amounts. Prior to the analyses, data were transformed for normalization.

Statistical analyses were run by Systat 13 (Systat Software, Inc., Chicago, IL, USA) using the GLM model for ANOVA and the multivariate analysis for the PCA.

### 3. Results

#### 3.1. Gas Exchanges and Pre-Dawn Water Potential

In the WDS, photosynthesis ( $A_{\text{net}}$ ) of poplar was higher in spring ( $17.7 \mu\text{mol CO}_2 \text{ m}^{-2} \text{ s}^{-1}$ ), with a reduction in summer ( $6.3 \mu\text{mol CO}_2 \text{ m}^{-2} \text{ s}^{-1}$ ,  $p < 0.01$ ) and no activity in autumn because of the leaf fall (Figure 1A). In the SDS,  $A_{\text{net}}$  was similar in spring and autumn (on average  $7.4 \mu\text{mol CO}_2 \text{ m}^{-2} \text{ s}^{-1}$ ), while a lower value was observed in summer ( $3.8 \mu\text{mol CO}_2 \text{ m}^{-2} \text{ s}^{-1}$ ,  $p < 0.05$ ; Figure 1B).

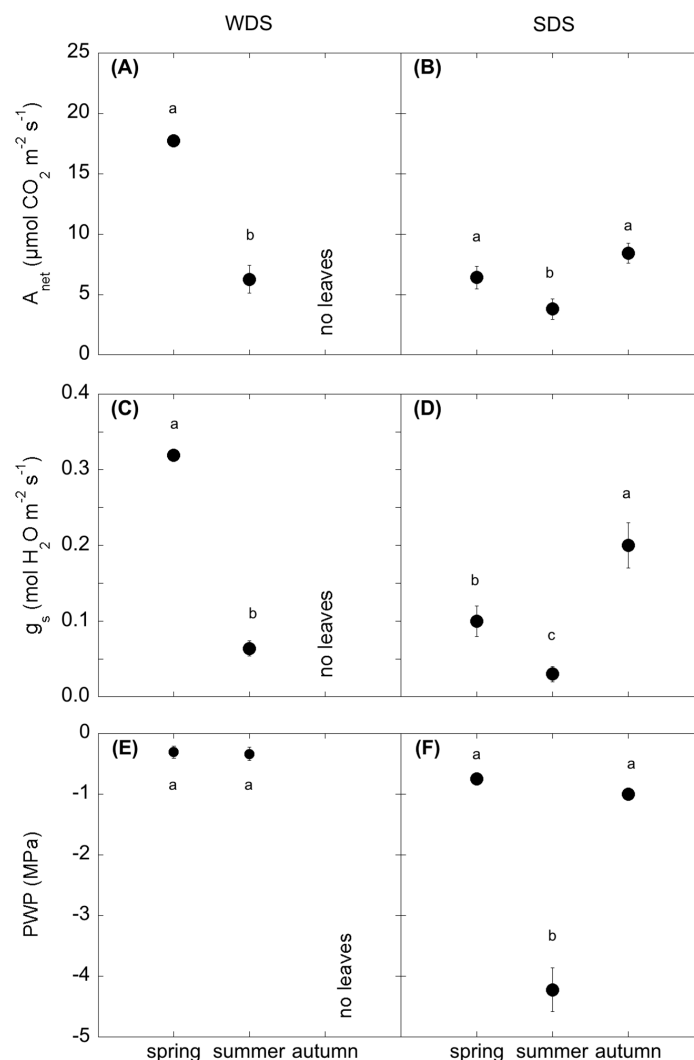


**Figure 1.** (A,B) assimilation rate ( $A \pm \text{s.e.}$ ;  $n = 10$ ); (C,D) stomatal conductance ( $g_s \pm \text{s.e.}$ ;  $n = 10$ ); (E,F) pre-dawn water potential (PWP  $\pm \text{s.e.}$ ;  $n = 10$ ) in the winter deciduous (WDS, left panels, A,C,E) and summer deciduous (SDS, right panels, B,D,F) sites. Gas exchange was not measured in autumn in the WDS site because of the leaf fall. Lowercase letters show significant differences among the seasons at  $p < 0.05$ .

In the WDS, significantly higher stomatal conductance ( $g_s$ ) was observed in spring ( $0.32 \text{ mol H}_2\text{O m}^{-2} \text{ s}^{-1}$ ,  $p < 0.01$ ) compared to summer ( $0.06 \text{ mol H}_2\text{O m}^{-2} \text{ s}^{-1}$ ; Figure 1C). In the SDS,  $g_s$  was significantly lower in summer ( $0.03 \text{ mol H}_2\text{O m}^{-2} \text{ s}^{-1}$ ) than in the other two seasons ( $p < 0.01$ ), while the maximum value was observed in autumn ( $0.2 \text{ mol H}_2\text{O m}^{-2} \text{ s}^{-1}$ ; Figure 1D).

In the WDS, the pre-dawn water potential (PWP) remained constant (on average  $-0.32 \text{ MPa}$ ) between the spring and the summer campaigns (Figure 1E). In the SDS, the lowest PWP value among the three seasons was measured in summer ( $-4.2 \text{ MPa}$ ,  $p < 0.001$ ), while in spring and autumn the PWP values were comparable ( $-0.9 \text{ MPa}$ ; Figure 1F).

### 3.2. Soil $\text{CO}_2$ Efflux

In the WDS site, soil  $\text{CO}_2$  efflux (SR) was on average  $1.8 \mu\text{mol CO}_2 \text{ m}^{-2} \text{ s}^{-1}$  in spring and summer, followed by a significant reduction in autumn ( $0.8 \mu\text{mol CO}_2 \text{ m}^{-2} \text{ s}^{-1}$ ,  $p < 0.01$ ; Figure 2A). The soil temperatures ( $T_s$ ) was 20, 37 and  $10 \text{ }^\circ\text{C}$ , respectively in spring, summer and autumn, coupled with soil water content (SWC) values of 7, 3, and 7% (Figure 2C).

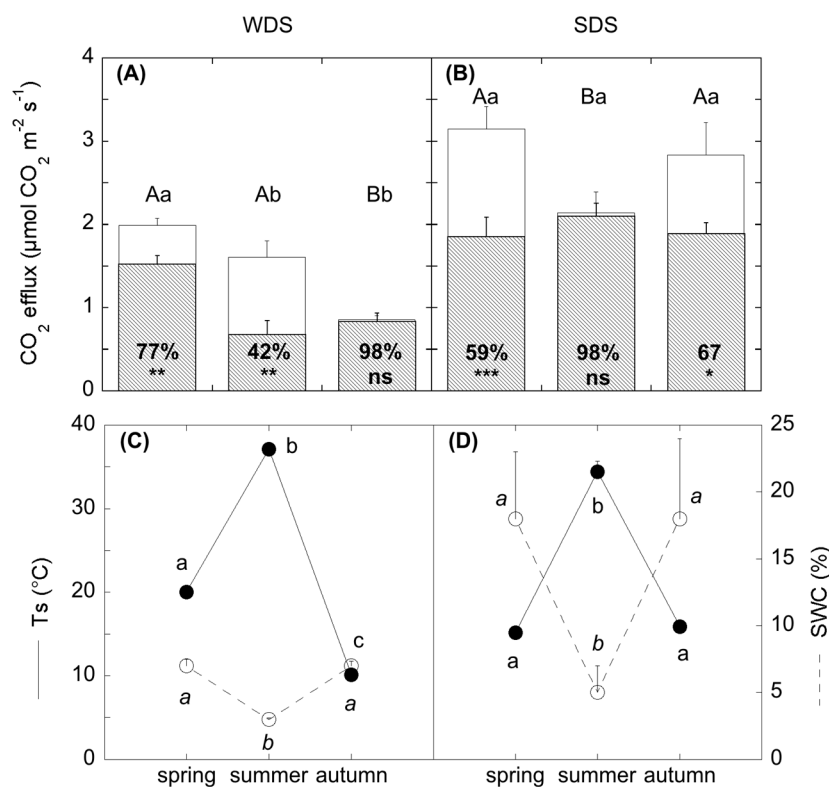


**Figure 2.**  $\text{CO}_2$  efflux ( $\pm$ s.e.,  $n = 10$ ; bars, upper panels), soil water content (SWC  $\pm$  s.e.;  $n = 10$ ; lower panels; right y-axis) and soil temperature ( $T_s \pm$  s.e.,  $n = 10$ ; lower panels; left y-axis; temperature is full circle with continuous line, soil water content is white circle with dashed line) in winter deciduous (WDS, left panels, A,C) and summer deciduous (SDS, right panels, B,D) sites. In panels (A) and (B), total (field measurements; white bars) and heterotrophic (laboratory measurements; strikethrough bars)  $\text{CO}_2$  efflux are shown; percentage numbers are the contribution of the heterotrophic respiration to the total soil  $\text{CO}_2$  efflux; \*\*\*, \*\*, \* indicate differences between total and heterotrophic respiration at  $p < 0.001$ ,  $p < 0.01$ ,  $p < 0.05$ , respectively. Capital and lowercase letters in panels (A,B) show significant seasonal variations ( $p < 0.05$ ) of total and heterotrophic  $\text{CO}_2$  efflux, respectively. In panels (C,D) normal and italic lowercase letters indicate seasonal differences of soil temperature and soil water content, respectively.

In the SDS, SR was similar in spring and autumn (on average  $3.0 \mu\text{mol CO}_2 \text{ m}^{-2} \text{ s}^{-1}$ ), while a lower value was observed in summer ( $2.1 \mu\text{mol CO}_2 \text{ m}^{-2} \text{ s}^{-1}$ ,  $p < 0.05$ ; Figure 2B). The  $T_s$  was 15, 34



and 16 °C respectively in spring, summer and autumn, coupled with SWC values of 18, 5 and 18% (Figure 2D).

In the WDS, heterotrophic respiration ( $SR_h$ ; Figure 2A) was at a maximum in spring ( $1.5 \mu\text{mol CO}_2 \text{ m}^{-2} \text{ s}^{-1}$ ), then significantly decreased to  $0.8 \mu\text{mol CO}_2 \text{ m}^{-2} \text{ s}^{-1}$  ( $p < 0.05$ ) by the following two sampling dates. In relative terms, autumn  $SR_h$  represented 98% of SR, while in spring and summer this contribution was 77% and 42%, respectively.

In the SDS,  $SR_h$  did not change among seasons being on average equal to  $2.0 \mu\text{mol CO}_2 \text{ m}^{-2} \text{ s}^{-1}$ . In relative terms, summer  $SR_h$  represented 98% of SR, while in spring and autumn this contribution was 59% and 67%, respectively (Figure 2B).

### 3.3. Heterotrophic Soil Basal Respiration and Temperature Sensitivity

In the WDS, a higher heterotrophic basal respiration ( $SR_b$ ; Figure 3A) was measured in spring ( $0.78 \mu\text{mol CO}_2 \text{ m}^{-2} \text{ s}^{-1}$ ,  $p < 0.05$ ), while similar values were observed in summer and autumn ( $0.5 \mu\text{mol CO}_2 \text{ m}^{-2} \text{ s}^{-1}$ ). The temperature sensitivity of the heterotrophic respiration ( $Q_{10}$ ; Figure 3C) was significantly higher in autumn (1.6,  $p < 0.05$ ) compared to summer (1.3), while in spring it was 1.4.

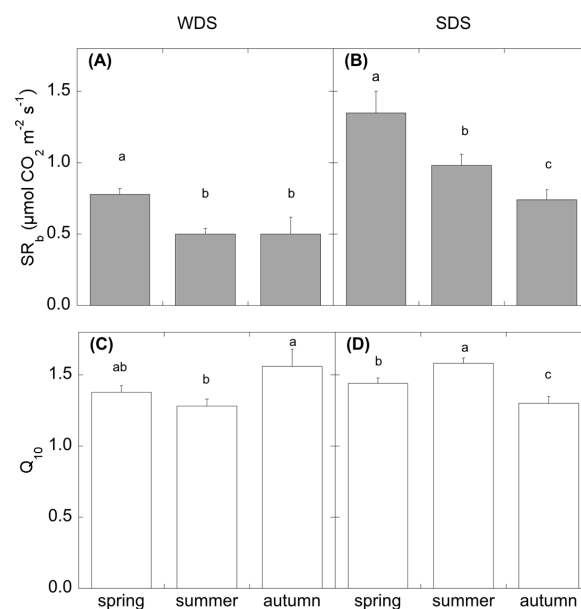


**Figure 3.** Heterotrophic soil basal respiration  $SR_b$  and temperature sensitivity  $Q_{10}$  calculated by fitting the exponential equation  $SR_h = a \cdot \exp(k \cdot Ts)$ .  $SR_b = a$  for  $Ts = 0 \text{ }^\circ\text{C}$ ,  $Q_{10} = \exp(10 \cdot k)$  in winter deciduous (WDS, left panels, A,C) and summer deciduous (SDS, right panels, B,D) sites. Lowercase letters show significant seasonal differences ( $p < 0.05$ ) in each site for each parameter ( $\pm$ s.e.,  $n = 10$ ).

In the SDS,  $SR_b$  (Figure 3B) was  $1.3 \mu\text{mol CO}_2 \text{ m}^{-2} \text{ s}^{-1}$  in spring.  $SR_b$  significantly dropped to about  $1 \mu\text{mol CO}_2 \text{ m}^{-2} \text{ s}^{-1}$  ( $p < 0.05$ ) and then to  $0.7 \mu\text{mol CO}_2 \text{ m}^{-2} \text{ s}^{-1}$  ( $p < 0.05$ ), respectively in summer and autumn. The  $Q_{10}$  (Figure 3D) was on average 1.4, spanning from the highest value in summer (1.6,  $p < 0.05$ ) to the minimum (1.3,  $p < 0.05$ ) in autumn.

### 3.4. C Pools

The C content in the topsoil (0–10 cm depth) was on average 0.74% and 3.8% respectively in the WDS and the SDS (data not shown).

In the WDS, the concentration of water-extractable organic carbon (WEOC) was higher in spring ( $66 \mu\text{g g}^{-1}$ ,  $p < 0.05$ ) and equally reduced in summer and autumn ( $40 \mu\text{g g}^{-1}$ ; Figure 4A). In the SDS, higher WEOC was measured in summer ( $88 \mu\text{g g}^{-1}$ ,  $p < 0.05$ ) compared to spring and autumn ( $38 \mu\text{g g}^{-1}$ ; Figure 4B). A positive correlation (not shown) between WEOC and the respiration measured

in laboratory ( $SR_h$ ) was observed in both sites (WDS:  $SR_h = 0.02 \cdot WEOC - 0.30$ ,  $R^2 = 0.94$ ,  $p < 0.001$ ; SDS:  $SR_h = 0.017 \cdot WEOC + 1.25$ ,  $R^2 = 0.93$ ,  $p < 0.001$ ).

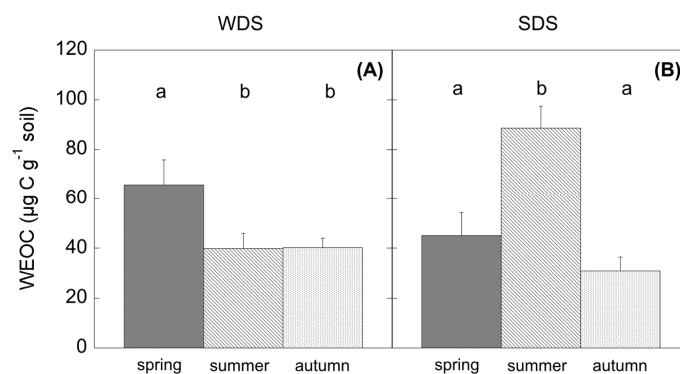


**Figure 4.** Water-extractable organic carbon ( $WEOC \pm$  s.e.) in winter deciduous (WDS) (A) and summer deciduous (SDS) (B) sites, during the three seasons. Different letters show significant differences ( $p < 0.05$ ) among the seasons. Spring = grey; Summer = dashed; Autumn = white.

### 3.5. Community Level Physiological Profiles (CLPP) Based on Substrate-Induced Respiration (SIR)

In the WDS, the induced respiration (SIR) by easily decomposable substrates (carbohydrates) did not change over time, being on average  $9.6 \mu\text{mol CO}_2 \text{ g}^{-1} \text{ h}^{-1}$  (Figure 5A). More complex and slowly decomposable substrates' respiration (carboxylic acids, amino acids and N-acetyl glucosamine) was higher in spring ( $10.3 \mu\text{mol CO}_2 \text{ g}^{-1} \text{ h}^{-1}$ ) than in summer and autumn ( $2.2 \mu\text{mol CO}_2 \text{ g}^{-1} \text{ h}^{-1}$ ,  $p < 0.01$ ). In summer, SIR by carbohydrates was higher than by other more complex substrates.

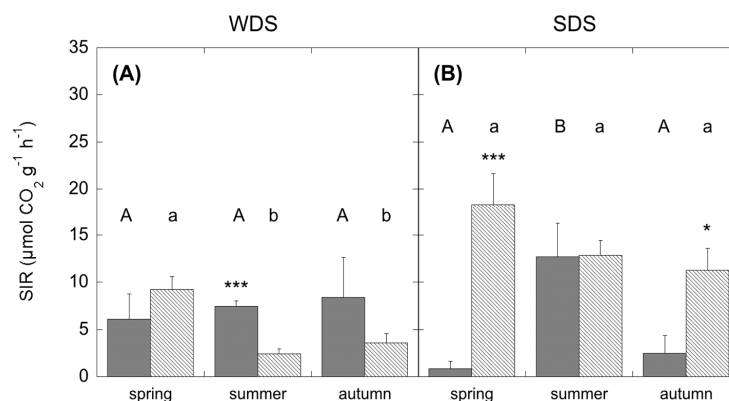


**Figure 5.** Substrate-induced respiration ( $SIR \pm$  s.e.) by easily decomposable substrates (Carbohydrates; grey bars) and more complex and slowly decomposable substrates (average of carboxylic acids, amino acids and N-acetyl glucosamine; dashed bars) in winter deciduous (WDS) (A) and summer deciduous (SDS) (B) sites. Capital letters show significant differences ( $p < 0.05$ ) among the seasons for SIR easily decomposable substrates; lowercase letters show significant differences ( $p < 0.05$ ) among the seasons for slowly decomposable substrates. Asterisks (\*\*\*, \* for  $p < 0.001$ , and  $p < 0.05$ , respectively) show significant differences between SIR by the easily decomposable and slowly decomposable substrates in each season.

In the SDS, SIR by carbohydrates showed a significant temporal dynamic (Figure 5B), with a higher flux in summer ( $15.8 \mu\text{mol CO}_2 \text{ g}^{-1} \text{ h}^{-1}$ ,  $p < 0.05$ ) and lower in spring and autumn ( $5.1 \mu\text{mol CO}_2 \text{ g}^{-1} \text{ h}^{-1}$ ). SIR by complex substrates was constant at the three sampling dates ( $14.8 \mu\text{mol CO}_2 \text{ g}^{-1} \text{ h}^{-1}$ ). Moreover, in spring and autumn SIR by complex substrates was higher compared to SIR by carbohydrates ( $p < 0.001$  and  $p < 0.05$  respectively).

The Principal Component Analysis (PCA) of the community level physiological profiles (CLPP; Figure 6A) showed a separation of microbial functional diversity in the WDS along Root 1 (mainly discriminating carbohydrates from the other substrates; Figure 6B), which accounted for 52% of the entire variability, with the spring samples grouping apart from the summer and autumn ones. In the SDS a separation was observed in three different groups.

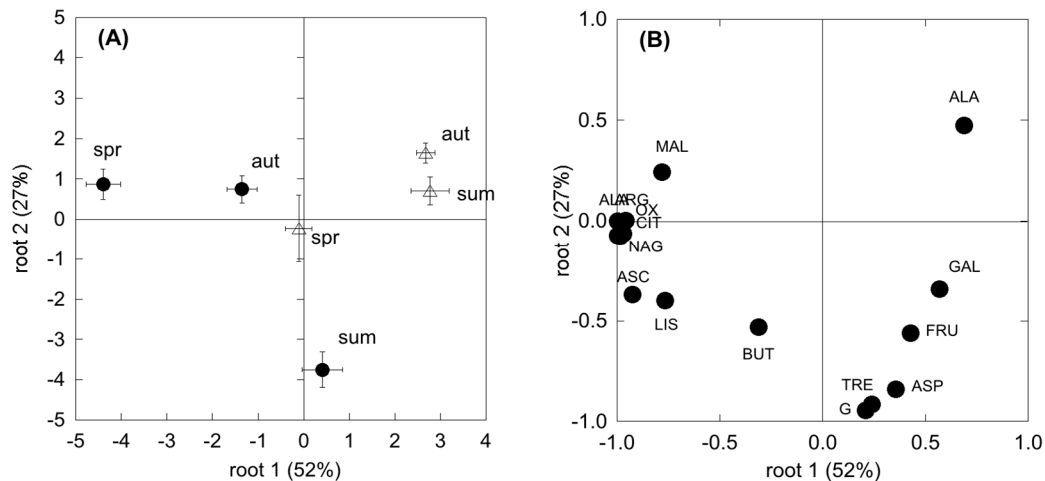


**Figure 6.** Principal Component Analysis (PCA) of the community level physiological profile (CLPP). (A) Factor coordinates of cases: empty triangles = WDS, full circles = SDS; Spr = spring, sum = Summer, aut = Autumn (B) factor loadings of variables; for labels see Table A2.

### 3.6. Microbial Community Composition by EL-FAME Characterization

In the WDS, the total amount of ester-linked fatty acid methyl ester (tot FAME) was on average  $0.16 \text{ nmol g}^{-1}$ , with a significant negative trend from spring to autumn (Table 3). Most of the EL-FAME (85% of the total) derived from bacteria. G+ showed a higher value in spring compared to both summer and autumn, differently from GRAM− dynamic which remained constant. Fungi were similar in spring and summer and then significantly decreased in autumn.

**Table 3.** Content of EL-FAME ( $\text{nmol g}^{-1}$  soil) along the seasons in winter deciduous (WDS) and summer deciduous (SDS) sites. Different lowercase letters mean significant ( $p < 0.05$ ) temporal variation in each group.

	WDS			SDS		
	Spring	Summer	Autumn	Spring	Summer	Autumn
total FAME	0.204 a	0.158 a	0.116 b	0.621 b	0.722 a	0.466 c
Total Bacteria	0.174 a	0.132 ab	0.102 b	0.516 b	0.613 a	0.367 c
G+	0.051 a	0.033 b	0.025 b	0.163 a	0.166 a	0.090 b
G−	0.046 a	0.034 a	0.033 a	0.138 a	0.114 ab	0.080 b
Actinomycetes	0.012 a	0.005 b	0.011 ab	0.033 a	0.031 a	0.021 b
Fungi	0.027 b	0.023 b	0.008 a	0.082 a	0.096 a	0.085 a
Protozoa	0.003 b	0.003 b	0.006 a	0.022 a	0.013 b	0.014 b

In the SDS, the tot FAME was significantly higher in summer and lower in autumn. The FAME from bacteria was about 82% of the total, with a significant lower amount in autumn compared to spring and summer (Table 3). G+ bacteria were equal in spring and summer and decreased in autumn; GRAM− showed an insignificant decreasing trend from spring to autumn. Fungi EL-FAME was on average  $0.09 \text{ nmol g}^{-1}$ , independently of the season (Table 3).

The PCA (Figure 7) showed a similar EL-FAME structure in all seasons in the WDS. In the SDS, the three seasons formed three different groups (Figure 7A). EL-FAME from the WDS and the SDS were different along Root 1. Root 1 grouped most of the different EL-FAMES, while two of them, characterizing Fungi, were distributed along Root 2 (Figure 7B).

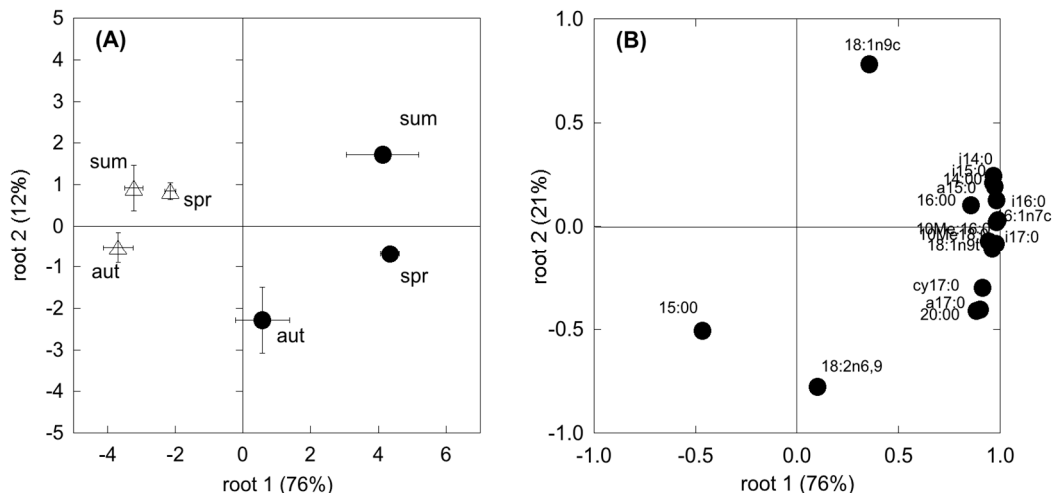


**Figure 7.** Principal Component Analysis (PCA) of microbial population structure based on the EL-FAME profiles. (A) Factor coordinates of cases: empty triangles = WDS, full circles = SDS; Spr = Spring; sum = Summer; aut = Autumn; (B) factor loadings of variables; for labels see Table A3.

SIR and total EL-FAME were both significantly mostly correlated with SR<sub>h</sub>, with the exception of carbohydrates and amino acids, and fungi and protozoa respectively (Table 4). SR showed significant correlation with the microbial degradation of carboxylic acids and N-acetyl glucosamine substrate and the G+, GRAM– and protozoa (Table 4). SIR and total FAME showed a high correlation (Table 4).

**Table 4.** Pearson coefficients of correlation between SR and SR<sub>h</sub> with SIR and EL-FAME parameters. \*  $p < 0.05$ ; \*\*  $p < 0.01$ ; \*\*\*  $p < 0.001$ ; n.s. = not significant.

	SR		SR <sub>h</sub>		SIR	
SIR	0.66	n.s.	0.92	**		
carbohydrates	-0.65	n.s.	-0.05	n.s.	-0.03	n.s.
carboxylic acids	0.91	**	0.79	*	0.83	*
amino acids	0.64	n.s.	0.88	n.s.	0.99	***
NAG	0.93	*	0.77	*	0.74	*
total FAME	0.68	n.s.	0.92	**	0.91	**
Total bacterial	0.70	n.s.	0.90	*	0.94	***
G+	0.72	*	0.87	*	0.96	***
G–	0.79	*	0.82	*	0.93	***
Actinomycetes	0.70	n.s.	0.88	***	0.96	***
Fungi	0.26	n.s.	0.65	n.s.	0.39	n.s.
Protozoa	0.78	*	0.70	n.s.	0.77	*

#### 4. Discussion

In ecosystems facing severe spells of drought, plant assimilation is strictly dependent on water availability [42–45], whose duration controls the length of the growing season [46–48]. In this study, photosynthesis showed a strong seasonal variation, as confirmed by the significant correlation of A<sub>net</sub> with the environmental variables (soil and air temperature and soil water content; Table A4) in both species. In both WDS and SDS, the highest assimilation rates were coupled with the highest stomatal conductance (g<sub>s</sub>), while summer A<sub>net</sub> was reduced due to a drop of g<sub>s</sub>. The summer drop

was consistently different for the two species, with a more evident shrink in poplar compared to *Cistus*, underlined by the higher correlation of  $A_{net}$  with SWC. This can be attributed to the different water use efficiency of the two species. In fact, poplar is a winter deciduous plant; it boosts its assimilation rates, at the expense of water control, during the more favourable period [49,50]. Differently, *C. monspeliensis*, a summer deciduous Mediterranean species, taking advantage of the autumn period to extend the growing season after the summer drought, adopts more constant and lower assimilation rates in order to minimize both water loss throughout the year and the unit cost of leaf production [51,52].

Soil water shortage also affected the relation between total belowground fluxes (SR) and soil temperature. In fact, the response of SR to summer drought was different in the two sites: in SDS, SR was reduced, while in WDS it did not change and was similar to spring values. This was evidenced by the SR-Ts correlation; (Table A5), that was significant in both sites, but with opposite signs. This difference was attributable to the concurrent reversed sign of the correlation SR-SWC, confirming the stronger role of SWC than the solely temperature in regulating SR in dry ecosystems subjected to drought. These results are in line with the most recent outcomes on SR modelling in ecosystems facing drought, pointing to include soil moisture, inversely related to soil temperature [53–55].

SR partitioning demonstrated a different response of the two components of SR (autotrophic and heterotrophic- $SR_h$ ) to summer drought. In WDS, although SR did not change,  $SR_h$  contribution halved spring values and compensated with higher autotrophic respiration, probably due to an increase in root activity to maintain constant leaf water potential under water shortage [56]. In SDS,  $SR_h$  did not change in summer and was comparable to spring values. This different dynamic of  $CO_2$  efflux partitioning under water shortage can be explained by factors other than aridity. These factors can be different in the two sites. In fact, Kuzyakov and Gavrichkova [24] reported that in plants with a high root allocation of photosynthates and during a period that is not water-limited, together with the climatic drivers, the direct effect of plant activity on soil respiration also has to be taken into account because of the close link between photosynthesis and rhizosphere processes [23,57]: photosynthesis supplies carbohydrates to roots, modulating substrates' availability to the rhizosphere. During summer in SDS, the *Cistus* plant community, unable to access deep water, moved to a dormant status in order to maintain turgor. This caused a reduction in photosynthates and substrate availability; however, the observed summer depression of SR was not due to a modification of  $SR_h$  but to the suppression of autotrophic respiration, as already similarly observed in other ecosystem types under drought [13,58,59], and  $SR_h$  accounted for almost 100% of SR. Concurrently, a significant increase in WEOC was observed, likely because of the high root mortality occurring in summer in Mediterranean ecosystems [60,61] and the simultaneous photodegradation of surface litter at high irradiance [62,63], which both release high amounts of C into the soil. At the same time, a change in the microbial community assemblage could be detected. In WDS, during summer the reduced assimilation was related to a decrease of  $SR_h$  and also coupled with limited substrate availability. In this case, WEOC, which is strictly connected to the release of root exudates [64] changed accordingly. As reflected by SIR analysis, summer microbial community in WDS was able to respire carbohydrates rather than more complex substrates. Thus, a reduction of fresh C from aboveground, because of low stomatal conductance and reduced phloem transport, negatively affected  $SR_h$ . In this case, substrate quality and quantity more than water availability can modulate  $CO_2$  release in this ecosystem. This result is further confirmed by autumn fluxes, showing low  $SR_h$  fluxes because of the leaf shedding and the absence of photosynthate production.

The drought season differently affected the temperature coefficient of the heterotrophic respiration ( $Q_{10}$ ). In WDS, the dry period corresponded with the lower  $Q_{10}$ , reflecting the low bacterial activity in this site reported by [65]. For SDS, the dry period corresponded to the higher  $Q_{10}$ , as was already observed by de Dato et al. [53]. Davidson and Janssens [66] reported that the decomposition of more complex substrates could likely lead to higher  $Q_{10}$ . In summer, when the microbial community is potentially able to feed on substrates more easily, the presence of root residues from root mortality might have acted as a priming effect, increasing the decomposition of more complex substrates (high  $Q_{10}$ ), thus compensating for the climatic constraint.

The composition of the microbial community may differ among plant communities and season, likely translating into functional shifts in microbial metabolic capacity. In the present study, CLPP and EL-FAME revealed a dynamic assemblage of microbial communities, as could be expected under seasonal drought cycles [30,67]. However, SDS revealed a more plastic and opportunistic behaviour of microbial community than the WDS. In fact, in the WDS there was a constant use of carbohydrates no matter the season. Differently, in the SDS the complex substrates' use was constant all through the year and higher than carbohydrate use in both spring and autumn. Since substrates like carboxylic acids, amino acids and glucosamine are considered to mainly derive from roots (exudates and tissue degradation) [64,68], higher belowground C allocation in dry Mediterranean ecosystems [69] determines microbial survival even with a low presence of photosynthates. This was further confirmed by a significant relationship between SR and the degradation of these substrates, which was shown to be mostly used by the microbial communities. In addition, the generally more complex and physiologically diverse microbial community at the Mediterranean site, evidenced by the higher FAME, determined a higher resilience to unfavourable climatic and edaphic conditions. Unexpectedly f [70], fungi were shown to be less involved in CO<sub>2</sub> production in these two ecosystems, suggesting a larger sensitivity to drought with respect to other microbial groups. However, microbial communities in SDS appeared to be more driven by fungi than in WDS, which points to the importance of these groups in Mediterranean ecosystems [71].

## 5. Conclusions

The microbial community is known to be able to adapt easily to varying environmental conditions. In this study, this plasticity appeared different in two sites with dissimilar plant community facing an evident dry season. More plastic and opportunistic behaviour of the soil microbial community was observed in a semi-deciduous Mediterranean ecosystem compared to a winter deciduous temperate shrubland. In the first case, the microbial community was less connected to plant activity and thus photosynthates, but more prone to take advantage of substrates, whatever their origin, in any season. In the second case, as the microbial composition and metabolism were driven by easily decomposable substrates, a reduction in plant photosynthetic activity (due to reduced stomatal conductance or leaf shedding) caused a decrease in heterotrophic respiration.

We can conclude that the response of soil CO<sub>2</sub> efflux to water limitation is not exclusively dependent on the climate and that this response is modulated by the degree of adaptation of both plants and the microbial community to drought.

**Acknowledgments:** This research was funded by the EU-funded infrastructure INCREASE (Grant agreement no. 227628).

**Author Contributions:** G.d.D., A.L. and P.D.A. conceived and designed the experiment; G.d.D., A.L., S.R.S., R.M., D.L., G.G. performed experiment and analyses; S.R.S. contributed reagents/materials; G.d.D. and A.L. analysed the data; G.d.D. wrote the paper. All authors commented on the manuscript.

**Conflicts of Interest:** The authors declare no conflict of interest.

Appendix

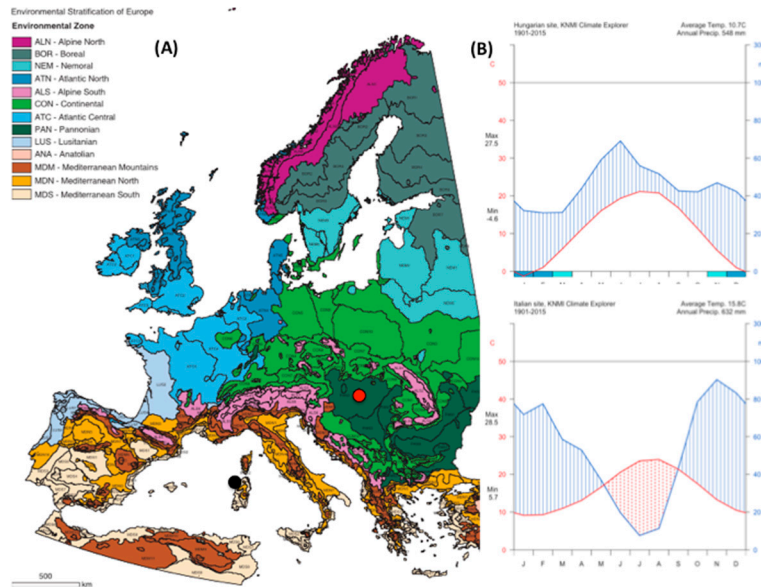


**Figure A1.** (A) Location of the study sites shown by the red and black dots for the Hungarian and Italian sites, respectively; the map is taken from Metzger et al. 2005; (B) Walther–Lieth diagrams of the long-term temperature and precipitation data (1901–2015, data from monthly CRU TS v.4.00, KNMI Climate Explorer <http://climexp.knmi.nl>, resolution 0.5 °C) for the Hungarian site (upper panel) and Italian site (lower panel).



(A)

**Figure A2.** *Cont.*



(B)

**Figure A2.** Details of the ecosystem types under investigation: (A) the Hungarian forest–steppe transitional biome (WDS); and (B) the Mediterranean shrubland (SDS).

**Table A1.** Microclimate conditions inside the cuvette during gas exchange measurements in the two study sites. T: leaf temperature; VPD: vapour pressure deficit; PAR: photosynthetic active radiation.

		T	VPD	PAR
		°C	kPa	$\mu\text{mol m}^{-2} \text{s}^{-1}$
WDS	spring	21.4	1.3	1300
	summer	36.5	3.7	2000
	autumn	-	-	-
SDS	spring	20.0	0.7	1200
	summer	33.0	3.3	2000
	autumn	19.1	0.8	1000

**Table A2.** Substrates used for CLPP analysis. Different amounts of delivered C depend on substrates' solubility in water.

Substrates	Type	Delivered ( $\text{mg mL}^{-1}$ )	Label
D-glucose	Carb	30	G
D-galactose	Carb	30	GAL
D-fructose	Carb	30	FRU
L-arabinose	Carb	30	ARA
Trehalose	Carb	0.3	TRE
Citric acid	CarbAc	30	CIT
Oxalic acid	CarbAc	7.5	OX
Ascorbic acid	CarbAc	30	ASC
Malic acid	CarbAc	0.3	MAL
Aspartic acid	AmAc	7.5	ASP
Lysine	AmAc	3	LIS
Alanine	AmAc	7.5	ALA
$\gamma$ -aminobutyric acid	AmAc	30	BUT
Arginine	AmAc	30	ARG
N-acetyl-glucosamine	amide	7.5	NAG

Carb: carbohydrates; CarbAc: Carboxylic acid; AmAc: Amino acid.



**Table A3.** Ester linked fatty acids (EL-FAMES) signature assignment used in this study.

Biomarkers	References
<i>Gram+</i>	
i 14:0	
i 15:0	
a 15:0	[72–77]
i 16:0	
i 17:0	
a 17:0	
<i>General</i>	
14:0	
15:0	[73–77]
16:0	
<i>Gram–</i>	
16:1 $\omega$ 7c	
Cy 17:0	[73–77]
18:1 $\omega$ 9t	
<i>Actinomycetes</i>	
10Me 16:0	
10Me18:0	[72,73,78]
<i>Fungi</i>	
18:1 $\omega$ 9c	
18:2 $\omega$ 6,9	[73,74,79]
<i>Protozoa</i>	
20:0	[80]

**Table A4.** Correlations table between the fluxes (SR and  $A_{net}$ ) with the climatic variables and the plant water status in the two sites. Bold values are significant at  $p < 0.05$ .

	WDS						
	SR	$A_{net}$	Ts	SWC	Ta	$g_s$	PWP
SR	1						
$A_{net}$	0.33	1					
Ts	<b>0.50</b>	<b>−0.91</b>	1				
SWC	<b>−0.42</b>	<b>0.91</b>	<b>−0.93</b>	1			
Ta	−0.36	<b>−0.90</b>	<b>0.99</b>	<b>−0.99</b>	1		
$g_s$	0.33	<b>0.93</b>	<b>−0.92</b>	<b>0.93</b>	<b>−0.93</b>	1	
PWP	−0.25	0.06	−0.15	0.14	−0.19	0.18	1
	SDS						
	SR	$A_{net}$	Ts	SWC	Ta	$g_s$	PWP
SR	1						
$A_{net}$	0.22	1					
Ts	<b>−0.49</b>	<b>−0.67</b>	1				
SWC	<b>0.56</b>	<b>0.49</b>	<b>−0.87</b>	1			
Ta	<b>−0.54</b>	<b>−0.65</b>	<b>0.96</b>	<b>0.91</b>	1		
$g_s$	0.16	<b>0.83</b>	<b>−0.72</b>	<b>0.64</b>	<b>−0.74</b>	1	
PWP	<b>0.53</b>	<b>0.59</b>	<b>−0.93</b>	<b>0.83</b>	<b>−0.91</b>	<b>0.66</b>	1

A = Assimilation; SR = soil CO<sub>2</sub> efflux; Ts = soil temperature; SWC = soil water content; Ta = air temperature;  $g_s$  = stomatal conductance; PWP = pre-dawn leaf water potential.

**Table A5.** Correlations table between the soil CO<sub>2</sub> emission, heterotrophic soil CO<sub>2</sub> emission, Q<sub>10</sub> and soil microclimatic variables in the two sites. Bold values are significant at  $p < 0.05$ .

WDS					
	SR	SR <sub>h</sub>	Q10	Ts	SWC
SR	1				
SR <sub>h</sub>	0.15	1			
Q10	0.30	0.18	1		
Ts	<b>0.50</b>	−0.27	<b>−0.44</b>	1	
SWC	<b>−0.42</b>	<b>0.51</b>	0.36	<b>−0.93</b>	1
SDS					
	SR	SR <sub>h</sub>	q10	Ts	SWC
SR	1				
SR <sub>h</sub>	−0.24	1			
Q10	−0.28	0.32	1		
Ts	<b>−0.49</b>	0.20	<b>0.57</b>	1	
SWC	<b>0.56</b>	−0.23	<b>−0.63</b>	<b>−0.96</b>	1

SR = soil CO<sub>2</sub> efflux; SR<sub>h</sub> = heterotrophic soil CO<sub>2</sub> efflux; Q<sub>10</sub> = temperature sensitivity of SR<sub>h</sub>; Ts = soil temperature; SWC = soil water content.

## References

- Knapp, A.K.; Beier, C.; Briske, D.D.; Classen, A.T.; Luo, Y.; Reichstein, M.; Smith, M.D.; Smith, S.D.; Bell, J.E.; Philip, A.; et al. Consequences of more extreme precipitation regimes for terrestrial ecosystems. *Bioscience* **2008**, *58*, 811–821. [[CrossRef](#)]
- Rambal, S.; Ourcival, J.M.; Joffre, R.; Mouillot, F.; Nouvellon, Y.; Reichstein, M.; Rocheteau, A. Drought controls over conductance and assimilation of a Mediterranean evergreen ecosystem: Scaling from leaf to canopy. *Glob. Chang. Biol.* **2003**, *9*, 1813–1824. [[CrossRef](#)]
- Granier, A.; Reichstein, M.; Bréda, N.; Janssens, I.A.; Falge, E.; Ciais, P.; Grunwald, T.; Aubinet, M.; Berbigier, P.; Bernhofer, C.; et al. Evidence for soil water control on carbon and water dynamics in European forests during the extremely dry year: 2003. *Agric. For. Meteorol.* **2007**, *143*, 123–145. [[CrossRef](#)]
- Mouillot, F.; Rambal, S.; Limousin, J.-M.; Longepierre, D.; Kheder-Chiraz, B.; Ouelhazi, B. Mediterranean ecosystems facing global change: Resilient or close to tipping point? In *The mediterranean Region under Climate Change—A Scientific Update*; Sabrie, M.-L., Gibert-Brunet, E., Mourier, T., Eds.; IRD Editions Institut De Recherche Pour Le Développement: Marseille, France, 2016.
- Sperlich, D.; Barbeta, A.; Ogaya, R.; Sabaté, S.; Peñuelas, J. Balance between carbon gain and loss under long-term drought: Impacts on foliar respiration and photosynthesis in *Quercus ilex* L. *J. Exp. Bot.* **2016**, *67*, 821–833. [[CrossRef](#)] [[PubMed](#)]
- Guidolotti, G.; De Dato, G.; Liberati, D.; De Angelis, P. Canopy Chamber: A useful tool to monitor the CO<sub>2</sub> exchange dynamics of shrubland. *iForest* **2017**, *10*, 597–604. [[CrossRef](#)]
- Reichstein, M.; Tenhunen, J.D.; Rouspard, O.; Ourcival, J.M.; Rambal, S.; Miglietta, F.; Peressotti, M.; Pecchiari, M.; Tirone, G.; Valentini, R. Severe drought effects on ecosystem CO<sub>2</sub> and H<sub>2</sub>O fluxes at three Mediterranean evergreen sites: Revision of current hypotheses? *Glob. Chang. Biol.* **2002**, *8*, 999–1017. [[CrossRef](#)]
- Reichstein, M.; Tenhunen, J.D.; Rouspard, O.; Ourcival, J.-M.; Rambal, S.; Dore, S.; Valentini, R. Ecosystem respiration in two Mediterranean evergreen holm Oak forest: Drought effects and decomposition dynamics. *Funct. Ecol.* **2002**, *16*, 27–39. [[CrossRef](#)]
- Chen, S.; Lin, G.; Huang, J.; Jenerette, D.G. Dependence of carbon sequestration on the differential responses of ecosystem photosynthesis and respiration to rain pulses in a semiarid steppe. *Glob. Chang. Biol.* **2009**, *15*, 2450–2461. [[CrossRef](#)]
- Bond-Lamberty, B.; Thomson, A. A global database of soil respiration data. *Biogeosciences* **2010**, *7*, 1915–1926. [[CrossRef](#)]

11. Kuzyakov, Y. Sources of CO<sub>2</sub> efflux from soil and review of partitioning methods. *Soil Biol. Biochem.* **2006**, *38*, 425–448. [[CrossRef](#)]
12. Hanson, P.J.; Edwards, N.T.; Garten, C.T.; Andrews, J.A. Separating root and soil microbial contributions to soil respiration: A review of methods and observations. *Biogeochemistry* **2000**, *48*, 115–146. [[CrossRef](#)]
13. Tang, J.; Baldocchi, D.D. Spatial–temporal variation in soil respiration in an oak–grass savanna ecosystem in California and its partitioning into autotrophic and heterotrophic components. *Biogeochemistry* **2005**, *73*, 183–207. [[CrossRef](#)]
14. Curiel Yuste, J.; Janssens, I.A.; Carrara, A.; Ceulemans, R. Annual Q<sub>10</sub> of soil respiration reflects plant phenological patterns as well as temperature sensitivity. *Glob. Chang. Biol.* **2004**, *10*, 161–169. [[CrossRef](#)]
15. Churchland, C.; Grayston, S.J.; Bengtson, P. Spatial variability of soil fungal and bacterial abundance: Consequences for carbon turnover along a transition from a forested to clear-cut site. *Soil Biol. Biochem.* **2013**, *63*, 5–13. [[CrossRef](#)]
16. Savage, K.; Davidson, E.A.; Tang, J. Diel patterns of autotrophic and heterotrophic respiration among phenological stages. *Glob. Chang. Biol.* **2013**, *19*, 1151–1159. [[CrossRef](#)] [[PubMed](#)]
17. Reth, S.; Reichstein, M.; Falge, E. The effect of soil water content, soil temperature, soil pH-value and the root mass on soil CO<sub>2</sub> efflux: A modified model. *Plant. Soil* **2005**, *268*, 21–33. [[CrossRef](#)]
18. Vargas, R.; Allen, M.F. Environmental controls and the influence of vegetation type, fine roots and rhizomorphs on diel and seasonal variation in soil respiration. *New Phytol.* **2008**, *179*, 460–471. [[CrossRef](#)] [[PubMed](#)]
19. Song, Q.-H.; Tan, Z.-H.; Zhang, Y.-P.; Cao, M.; Sha, L.-Q.; Tang, Y.; Liang, N.-S.; Schaefer, D.; Zhao, J.-F.; Zhao, J.-B.; et al. Spatial heterogeneity of soil respiration in a seasonal rainforest with complex terrain. *iForest Biogeosc. For. iForest* **2013**, *6*, 65–72. [[CrossRef](#)]
20. de Vries, F.T.; Manning, P.; Tallwin, J.R.B.; Mortimer, S.R.; Pilgrim, E.S.; Harrison, K.A.; Hobbs, P.J.; Quirk, H.; Shipley, B.; Cornelissen, J.H.C.; et al. Abiotic drivers and plant traits explain landscape-scale patterns in soil microbial communities. *Ecol. Lett.* **2012**, *15*, 1230–1239. [[CrossRef](#)] [[PubMed](#)]
21. Scott-Denton, L.E.; Rosenstiel, T.N.; Monson, R.K. Differential controls by climate and substrate over the heterotrophic and rhizospheric components of soil respiration. *Glob. Chang. Biol.* **2006**, *12*, 205–216. [[CrossRef](#)]
22. De Graaff, M.-A.; Classen, A.T.; Castro, H.F.; Schadt, C.W. Labile soil carbon inputs mediate the soil microbial community composition and plant residue decomposition rates. *New Phytol.* **2010**, *188*, 1055–1064. [[CrossRef](#)] [[PubMed](#)]
23. Högberg, P.; Nordgren, A.; Buchmann, N.; Taylor, A.F.S.; Ekblad, A.; Högberg, M.N.; Nyberg, G.; Ottosson-Löfvenius, M.; Read, D.J. Large-scale forest girdling shows that current photosynthesis drives soil respiration. *Nature* **2001**, *411*, 789–792. [[CrossRef](#)] [[PubMed](#)]
24. Kuzyakov, Y.; Gavrichkova, O. Time lag between photosynthesis and carbon dioxide efflux from soil: A review of mechanisms and controls. *Glob. Chang. Biol.* **2010**, *16*, 3386–3406. [[CrossRef](#)]
25. Subke, J.-A.; Voke, N.R.; Leronni, V.; Garnett, M.H.; Ineson, P. Dynamics and pathways of autotrophic and heterotrophic soil CO<sub>2</sub> efflux revealed by forest girdling. *J. Ecol.* **2010**, *99*, 186–193. [[CrossRef](#)]
26. Collins, S.L.; Sinsabaugh, R.L.; Crenshaw, C.; Green, L.; Porras-Alfaro, A.; Stursova, M.; Zeglin, L.H. Pulse dynamics and microbial processes in aridland ecosystems. *J. Ecol.* **2008**, *96*, 413–420. [[CrossRef](#)]
27. Fuchslueger, L.; Bahn, M.; Fritz, K.; Hasibeder, R.; Richter, A. Experimental drought reduces the transfer of recently fixed plant carbon to soil microbes and alters the bacterial community composition in a mountain meadow. *New Phytol.* **2014**, *201*, 916–927. [[CrossRef](#)] [[PubMed](#)]
28. Allison, S.D.; Martiny, J.B.H. Resistance, resilience, and redundancy in microbial communities. *Proc. Natl. Acad. Sci. USA* **2008**, *105*, 11512–11519. [[CrossRef](#)] [[PubMed](#)]
29. Bell, C.W.; Tissue, D.T.; Loik, M.E.; Wallenstein, M.D.; Acosta-Martinez, V.; Erickson, R.A.; Zak, J.C. Soil microbial and nutrient responses to 7 years of seasonally altered precipitation in a Chihuahuan Desert grassland. *Glob. Chang. Biol.* **2014**, *20*, 1657–1673. [[CrossRef](#)] [[PubMed](#)]
30. Wasserstrom, H.; Kublik, S.; Wasserstrom, R.; Schulz, S.; Schloter, M.; Steinberger, Y. Bacterial community composition in coastal dunes of the Mediterranean along a gradient from the sea shore to the inland. *Sci. Rep.* **2017**, *7*, 40266. [[CrossRef](#)] [[PubMed](#)]
31. Evans, S.E.; Wallenstein, M.D. Soil microbial community response to drying and rewetting stress: Does historical precipitation regime matter? *Biogeochemistry* **2012**, *109*, 101–116. [[CrossRef](#)]

32. Cleveland, C.C.; Nemergut, D.R.; Schmidt, S.K.; Townsend, A.R. Increases in soil respiration following labile carbon additions linked to rapid shifts in soil microbial community composition. *Biogeochemistry* **2007**, *82*, 229–240. [[CrossRef](#)]
33. Garcia-Pausas, J.; Paterson, E. Microbial community abundance and structure are determinants of soil organic matter mineralisation in the presence of labile carbon. *Soil Biol. Biochem.* **2011**, *43*, 1705–1713. [[CrossRef](#)]
34. Whitaker, J.; Ostle, N.; Nottingham, A.T.; Ccahuana, A.; Salinas, N.; Bardgett, R.D.; Meir, P.; McNamara, N.P. Microbial community composition explains soil respiration responses to changing carbon inputs along an Andes-to-Amazon elevation gradient. *J. Ecol.* **2014**, *102*, 1058–1071. [[CrossRef](#)] [[PubMed](#)]
35. Li, Y.; Liu, Y.; Wu, S.; Niu, L.; Tian, Y. Microbial properties explain temporal variation in soil respiration in a grassland subjected to nitrogen addition. *Sci. Rep.* **2015**, *5*, 18496. [[CrossRef](#)] [[PubMed](#)]
36. Curiel Yuste, J.; Fernandez-Gonzalez, A.J.; Fernandez-Lopez, M.; Ogaya, R.; Penuelas, J.; Sardans, J.; Lloret, F. Strong functional stability of soil microbial communities under semiarid Mediterranean conditions and subjected to long-term shifts in baseline precipitation. *Soil Biol. Biochem.* **2014**, *69*, 223–233. [[CrossRef](#)]
37. SardegnaARPA. Available online: [http://gis.sar.sardegna.it/gfmaplet/?map=carta\\_bioclimatica](http://gis.sar.sardegna.it/gfmaplet/?map=carta_bioclimatica) (accessed on 7 July 2017).
38. Metzger, M.J.; Bunce, R.G.H.; Jongman, R.H.G.; Muecher, C.A.; Watkins, J.W. A climatic stratification of the environment of Europe: A climatic stratification of the European environment. *Glob. Ecol. Biogeogr.* **2005**, *14*, 549–563. [[CrossRef](#)]
39. Lagomarsino, A.; De Angelis, P.; Moscatelli, M.C.; Grego, S. The influence of temperature and labile C substrates on heterotrophic respiration in response to elevated CO<sub>2</sub> and nitrogen fertilization. *Plant. Soil* **2009**, *317*, 223–234. [[CrossRef](#)]
40. Campbell, C.D.; Chapman, S.J.; Cameron, C.M.; Davidson, M.S.; Potts, J.M. A rapid microtiter plate method to measure carbon dioxide evolved from carbon substrate amendments so as to determine the physiological profiles of soil microbial communities by using whole soil. *Appl. Environ. Microbiol.* **2003**, *69*, 3593–3599. [[CrossRef](#)] [[PubMed](#)]
41. Schutter, M.E.; Dick, R.P. Comparison of Fatty Acid Methyl Ester (FAME) Methods for Characterizing Microbial Communities. *Soil Sci. Soc. Am. J.* **2000**, *64*, 1659–1668. [[CrossRef](#)]
42. Chaves, M.M.; Pereira, J.S.; Maroco, J.; Rodrigues, M.L.; Ricardo, C.P.P.; Osório, M.L.; Carvalho, I.; Faria, T.; Pinheiro, C. How plants cope with water stress in the field? Photosynthesis and growth. *Ann. Bot.* **2002**, *89*, 907–916. [[CrossRef](#)] [[PubMed](#)]
43. Flexas, J.; Diaz-Espejo, A.; Gago, J.; Gallé, A.; Galmés, J.; Gulías, J.; Medrano, H. Photosynthetic limitations in Mediterranean plants: A review. *Environ. Exp. Bot.* **2014**, *103*, 12–23. [[CrossRef](#)]
44. Limousin, J.M.; Bickford, C.P.; Dickman, L.T.; Pangle, R.E.; Hudson, P.J.; Boutz, A.L.; Gehres, N.; Osuna, J.L.; Pockman, W.T.; McDowell, N.G. Regulation and acclimation of leaf gas exchange in a pinon-juniper woodland exposed to three different precipitation regimes. *Plant Cell Environ.* **2013**, *36*, 1812–1825. [[CrossRef](#)] [[PubMed](#)]
45. Grassi, G.; Magnani, F. Stomatal, mesophyll conductance and biochemical limitations to photosynthesis as affected by drought and leaf ontogeny in ash and oak trees. *Plant Cell Environ.* **2005**, *28*, 834–849. [[CrossRef](#)]
46. Barbeta, A.; Ogaya, R.; Penuelas, J. Dampening effects of long-term experimental drought on growth and mortality rates of a Holm oak forest. *Glob. Chang. Biol.* **2013**, *19*, 3133–3144. [[CrossRef](#)] [[PubMed](#)]
47. Hoover, D.L.; Rogers, B.M. Not all droughts are created equal: The impacts of interannual drought pattern and magnitude on grassland carbon cycling. *Glob. Chang. Biol.* **2015**, *22*. [[CrossRef](#)] [[PubMed](#)]
48. Swidrak, I.; Schuster, R.; Oberhuber, W. Comparing growth phenology of co-occurring deciduous and evergreen conifers exposed to drought. *Flora* **2013**, *208*, 609–617. [[CrossRef](#)]
49. Ripullone, F.; Lauteri, M.; Grassi, G.; Amato, M.; Borghetti, M. Variation in nitrogen supply changes water-use efficiency of *Pseudotsuga menziesii* and *Populus x euroamericana*; a comparison of three approaches to determine water-use efficiency. *Tree Physiol.* **2004**, *24*, 671–679. [[CrossRef](#)] [[PubMed](#)]
50. Fichot, R.; Laurans, F.; Monclus, R.; Moreau, A.; Pilate, G.; Brignolas, F. Xylem anatomy correlates with gas exchange, water-use efficiency and growth performance under contrasting water regimes: Evidence from *Populus deltoides* x *Populus nigra* hybrids. *Tree Physiol.* **2009**, *29*, 1537–1549. [[CrossRef](#)] [[PubMed](#)]
51. Marty, C.; Lamaze, T.; Pornon, A. Leaf life span optimizes annual biomass production rather than plant photosynthetic capacity in an evergreen shrub. *New Phytol.* **2010**, *187*, 407–416. [[CrossRef](#)] [[PubMed](#)]

52. De Dato, G.D.; Micali, M.; Abou Jaoudé, R.; Liberati, D.; De Angelis, P. Earlier summer drought affects leaf functioning of the Mediterranean species *Cistus monspeliensis* L. *Environ. Exp. Bot.* **2013**, *93*, 13–19. [[CrossRef](#)]
53. de Dato, G.; De Angelis, P.; Sirca, C.; Beier, C. Impact of drought and increasing temperatures on soil CO<sub>2</sub> emissions in a Mediterranean shrubland (*gariga*). *Plant. Soil* **2010**, *327*, 153–166. [[CrossRef](#)]
54. Lellei-Kovács, E.; Botta-Dukát, Z.; de Dato, G.; Estiarte, M.; Guidolotti, G.; Kopittke, G.R.; Kovács-Láng, E.; Kröel-Dulay, G.; Larsen, K.S.; Peñelas, J.; et al. Temperature Dependence of Soil Respiration Modulated by Thresholds in Soil Water Availability Across European Shrubland Ecosystems. *Ecosystems* **2016**, *19*, 1460–1477. [[CrossRef](#)]
55. Carey, J.C.; Tang, J.; Templer, P.H.; Kroeger, K.D.; Crowther, T.W.; Burton, A.J.; Dukes, J.S.; Emmett, B.; Frey, S.D.; Heskel, M.A.; et al. Temperature response of soil respiration largely unaltered with experimental warming. *Proc. Natl. Acad. Sci. USA* **2016**, *113*, 13797–13802. [[CrossRef](#)] [[PubMed](#)]
56. Steudle, E. Water uptake by roots: Effects of water deficit. *J. Exp. Bot.* **2000**, *51*, 1531–1542. [[CrossRef](#)] [[PubMed](#)]
57. Högberg, P.; Högberg, M.N.; Göttlicher, S.G.; Betson, N.R.; Keel, S.G.; Metcalfe, D.B.; Campbell, C.; Schindlbacher, A.; Hurry, V.; Lundmark, T.; et al. High temporal resolution tracing of photosynthate carbon from the tree canopy to forest soil microorganisms. *New Phytol.* **2008**, *177*, 220–228. [[CrossRef](#)] [[PubMed](#)]
58. Balogh, J.; Papp, M.; Pintér, K.; Fóti, S.; Posta, K.; Eugster, W.; Nagy, Z. Autotrophic component of soil respiration is repressed by drought more than the heterotrophic one in dry grasslands. *Biogeosciences* **2016**, *13*, 5171–5182. [[CrossRef](#)]
59. Risk, D.; Nickerson, N.; Phillips, C.L.; Kellman, L.; Moroni, M. Drought alters respired  $\delta^{13}$  CO<sub>2</sub> from autotrophic, but not heterotrophic soil respiration. *Soil Biol. Biochem.* **2012**, *50*, 26–32. [[CrossRef](#)]
60. López, B.; Sabaté, S.; Gracia, C. Fine roots dynamics in a Mediterranean forest: Effects of drought and stem density. *Tree Physiol.* **1998**, *8*, 601–606. [[CrossRef](#)]
61. López, B.; Sabaté, S.; Gracia, C.A. Annual and seasonal changes in fine root biomass of a *Quercus. ilex* L. forest. *Plant. Soil* **2001**, *230*, 125–134. [[CrossRef](#)]
62. Rey, A. Mind the gap: Non-biological processes contributing to soil CO<sub>2</sub> efflux. *Glob. Chang. Biol.* **2015**, *21*, 1752–1761. [[CrossRef](#)] [[PubMed](#)]
63. Gliksmann, D.; Rey, A.; Seligmann, R.; Dumbur, R.; Sperling, O.; Navon, Y.; Haenel, S.; De Angelis, P.; Arnone, J.A.; Grünzweig, J.M. Biotic degradation at night, abiotic degradation at day: Positive feedbacks on litter decomposition in drylands. *Glob. Chang. Biol.* **2017**, *23*, 1564–1574. [[CrossRef](#)] [[PubMed](#)]
64. Jones, D.; Nguyen, C.; Finlay, R. Carbon flow in the rhizosphere: Carbon trading at the soil–root interface. *Plant. Soil* **2009**, *321*, 5–33. [[CrossRef](#)]
65. Lellei-Kovács, E.; Kovács-Láng, E.; Botta-Dukát, Z.; Kalapos, T.; Emmett, B.; Beier, C. Thresholds and interactive effects of soil moisture on the temperature response of soil respiration. *Eur. J. Soil Biol.* **2011**, *47*, 247–255. [[CrossRef](#)]
66. Davidson, E.A.; Janssens, I.A. Temperature sensitivity of soil carbon decomposition and feedbacks to climate change. *Nature* **2006**, *440*, 165–173. [[CrossRef](#)] [[PubMed](#)]
67. Waldrop, M.; Firestone, M. Seasonal dynamics of microbial community composition and function in oak canopy and open grassland soils. *Microb. Ecol.* **2006**, *52*, 470–479. [[CrossRef](#)] [[PubMed](#)]
68. Baudoin, E.; Benizri, E.; Guckert, A. Impact of artificial root exudates on the bacterial community structure in bulk soil and maize rhizosphere. *Soil Biol. Biochem.* **2003**, *35*, 1183–1192. [[CrossRef](#)]
69. Almagro, M.; LÚpez, J.; Boix-Fayos, C.; Albaladejo, J.; Martínez-Mena, M. Belowground carbon allocation patterns in a dry Mediterranean ecosystem: A comparison of two models. *Soil Biol. Biochem.* **2010**, *42*, 1549–1557. [[CrossRef](#)]
70. Manzoni, S.; Schimel, J.P.; Porporato, A. Responses of soil microbial communities to water stress: Results from a meta-analysis. *Ecology* **2012**, *93*, 930–938. [[CrossRef](#)] [[PubMed](#)]
71. Yuste, J.C.; Peñuelas, J.; Estiarte, M.; Garcia-Mas, J.; Mattana, S.; Ogaya, R.; Pujol, M.; Sardans, J. Drought-resistant fungi control soil organic matter decomposition and its response to temperature. *Glob. Chang. Biol.* **2011**, *17*, 1475–1486. [[CrossRef](#)]
72. Bååth, E.; Frostegård, Å.; Fritze, H. Soil bacterial biomass, activity, phospholipid fatty acid pattern, and pH tolerance in an area polluted with alkaline dust deposition. *Appl. Environ. Microbiol.* **1992**, *58*, 4026–4031. [[PubMed](#)]

73. Frostegård, A.; Tunlid, A.; Baath, E. Phospholipid fatty acid composition, biomass, and activity of microbial communities from two soil types experimentally exposed to different heavy metals. *Appl. Environ. Microbiol.* **1993**, *59*, 3605–3617. [[PubMed](#)]
74. Zelles, L. Phospholipid fatty acid profiles in selected members of soil microbial communities. *Chemosphere* **1997**, *35*, 275–294. [[CrossRef](#)]
75. Zogg, G.P.; Zak, D.R.; Ringelberg, D.B.; White, D.C.; Macdonald, N.W.; Pregitzer, K.S. Compositional and functional shifts in microbial communities due to soil warming. *Soil. Sci. Soc. Am. J.* **1997**, *61*, 475–481. [[CrossRef](#)]
76. Waldrop, M.P.; Balsler, T.C.; Firestone, M.K. Linking microbial community composition to function in a tropical soil. *Soil Biol. Biochem.* **2000**, *32*, 1837–1846. [[CrossRef](#)]
77. Fierer, N.; Schimel, J.P.; Holden, P.A. Variations in microbial community composition through two soil depth profiles. *Soil Biol. Biochem.* **2003**, *35*, 167–176. [[CrossRef](#)]
78. Allison, V.; Yermakov, Z.; Miller, R.; Jastrow, J.; Matamala, R. Using landscape and depth gradients to decouple the impact of correlated environmental variables on soil microbial community composition. *Soil Biol. Biochem.* **2007**, *39*, 505–516. [[CrossRef](#)]
79. Federle, T.W. Microbial distribution in soil—new techniques. In *Perspectives in Microbial Ecology*; Megusar, F., Gantar, M., Eds.; Slovene Society for Microbiology: Ljubljana, Slovenia, 1986; pp. 493–498.
80. White, D.C.; Stair, J.O.; Ringelberg, D.B. Quantitative comparisons of in situ microbial biodiversity by signature biomarker analysis. *J. Ind. Microbiol.* **1996**, *17*, 185–196. [[CrossRef](#)]



© 2017 by the authors. Licensee MDPI, Basel, Switzerland. This article is an open access article distributed under the terms and conditions of the Creative Commons Attribution (CC BY) license (<http://creativecommons.org/licenses/by/4.0/>).